RSC Advances

PAPER

View Article Online
View Journal | View Issue

Cite this: *RSC Adv.*, 2017, **7**, 6988

Stimuli-responsive magneto-/electro-chromatic color-tunable hydrophobic surface modified Fe_3O_4@SiO_2 core–shell nanoparticles for reflective display approaches

S. Lee,†[ab] J. Y. Kim,†[a] S. Cheon,[a] S. Kim,[a] D. Kim[b] and H. Ryu*[a]

Received 30th November 2016
Accepted 5th January 2017

DOI: 10.1039/c6ra27540k

www.rsc.org/advances

In order to provide stimuli-responsive properties under magnetic- and electric-forces enabling reflective color-changes in a liquid medium, the surface of silica coated-iron oxide core–shell nanoparticles (Fe_3O_4@SiO_2) is successfully modified with two-different types of silane coupling agents to improve the dispersion stability as well as the color change strength as a result of the effectively increased repulsion. A stimuli-responsive magneto- and electro-chromatic ink is prepared by mixing hydrophobic surface modified Fe_3O_4@SiO_2-Fx (x = 0 and 13) core–shell nanoparticles and a dispersing agent in a low dielectric medium (LDM). The magneto-chromatic and electro-chromatic stimuli-responsive properties are visually confirmed. Moreover, the optical reflective color spectra and color gamut calculated from the CIE chromaticity coordinates of the hydrophobic surface modified Fe_3O_4@SiO_2-F13 core–shell nanoparticles (with "F moiety" in the molecular structure) under an applied voltage range of 0 V to 10 V show that the hydrophobic surface modified magnetite nanoparticles are promising candidates for reflective display applications.

Introduction

In recent years, it has become more important to develop a display technology which can show dynamic and visible information data. There are two display methods: one method is an emissive display commonly referred to as organic light-emitting devices (OLEDs) emitting the light itself,[1,2] and the other method is a reflective display mostly referred to as liquid crystal devices (LCDs) reflecting the incident light.[3] Both displays are widely used throughout our lives and by various industries.

Between the two display methods, reflective displays[4] with the advantages of low power, high resolution, and not requiring a backlight have more merit for electrophoretic displays (EPDs),[5] electrochromic displays (ECDs),[6] and electrowetting displays (EWDs).[7]

However, those reflective devices have major drawbacks in terms of easily and simply changing colors with a clear color-chromaticity. In order to overcome and solve these drawbacks, there is a reflective color-change system by controlling the nanoparticle–nanoparticle distance under magnetic and electric stimuli, which is well-known as the photonic crystal phenomenon. The photonic crystal (Phc) phenomenon can be observed when a specific distance among nanoparticles is matched to a particular wavelength of the incident light.[8–11]

Magnetite (Fe_3O_4) nanoparticles have gained much attention due to their existing Phc phenomenon even though Fe_3O_4 nanoparticles have been widely used in the biomedical field.[12–14] Many of the investigations of the Phc phenomenon have been in a liquid medium in which the diffraction wavelength can be varied by influencing the strength of the external stimuli causing colloidal movement, resulting in possibly tunable optical transmittance[15–17] and reflective colors.[18–20]

Generally, Phc colloidal arrays in a liquid medium are primarily generated by electrostatic force, and Phc colloidal arrays with varying distances are mainly controlled by external stimuli such as magnetic and electric fields, which are well suited for approaches using reflective displays.[21] Because the Fe_3O_4 nanoparticles have better movement in a liquid medium compared to being dispersed in a film, the surface of Fe_3O_4 nanoparticles is an essential factor. Typically, the surface of Fe_3O_4 nanoparticles is modified to be hydrophilic for *in vivo* and *in vitro* applications.[22] However, in terms of an electric stimuli-response, a non-aqueous medium with a low dielectric property is absolutely necessary to effectively move Fe_3O_4 nanoparticles. The surface modification of the Fe_3O_4 nanoparticles should be done with hydrophobic capping molecules which are expected to provide enhanced dispersion stability and sufficient

[a]*Reality Display Device Research Section, Electronics and Telecommunications Research Institute (ETRI), 218 Gajeong-ro, Yuseong-gu, 34129 Daejeon, Korea. E-mail: hjryu@etri.re.kr; jooyeon.kim@etri.re.kr*

[b]*College of Electronics and Information Engineering, Sejong University, 209 Neungdong-ro, Gwangjin-gu, 05006 Seoul, Korea*

† S. Lee and J. Y. Kim contributed equally to this work.

repulsive inter-actions between the surface modified Fe_3O_4 nanoparticles. In order to compare the magneto-/electro-chromatic properties of hydrophobic surface modified Fe_3O_4 nanoparticles, two-different types of silane coupling agents were selected and attached to silica-coated Fe_3O_4 (Fe_3O_4@SiO_2) core–shell nanoparticles which provide an easier synthetic route to vary the surface modification than bare Fe_3O_4. In this work, therefore, the dispersion stability and the color-change strength of two-different hydrophobic surface modified Fe_3O_4@SiO_2-Fx (x = 0 and 13, referred to as Fe_3O_4@SiO_2-F0 and Fe_3O_4@SiO_2-F13) core–shell nanoparticles were compared with a "no F moiety" and "F moiety" in the hydrophobic capping molecular structures. The related results indicate a more hydrophobic condition with the "F moiety" in the hydrophobic capping molecular structures on Fe_3O_4@SiO_2-Fx.

Results and discussion

In modifying the surface with two-different types of silane coupling agents, the surface modification route is shown for the Fe_3O_4@SiO_2 core–shell nanoparticles in Scheme 1. The overall surface modification processes were as follows: ultrasonic radiation of the dried Fe_3O_4@SiO_2 core–shell nanoparticles mixed into a base solvent, controlling the pH to be 11 by adding NH_3 solution and then two-different types of silane coupling agents (referred to as F0-OTS and F13-OTS) added into the reactor. Then, two-different hydrophobic surface modified Fe_3O_4@SiO_2 core–shell nanoparticles, referred to as Fe_3O_4@SiO_2-F0 and Fe_3O_4@SiO_2-F13, were obtained.

In order to determine the surface modification, the chemical species of the two-different hydrophobic surface modified Fe_3O_4@SiO_2-F0 and Fe_3O_4@SiO_2-F13 core–shell nanoparticles prepared as a powder were analyzed by XPS. As seen in Fig. 1,

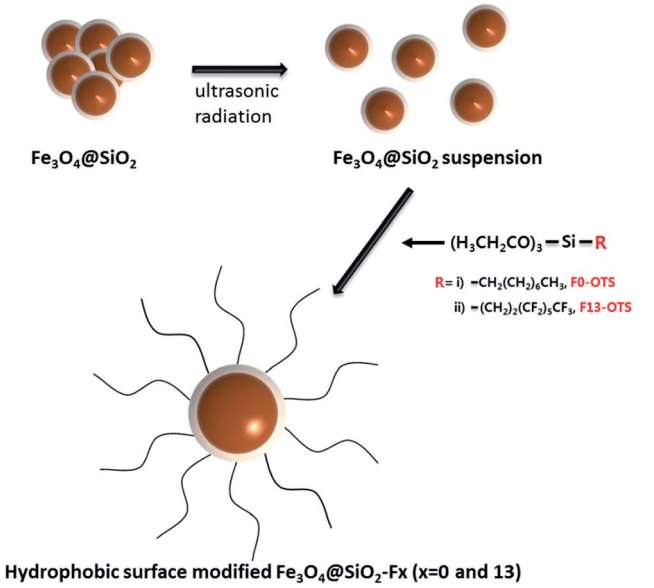

Scheme 1 Schematic showing the hydrophobic surface modification of the Fe_3O_4@SiO_2 core–shell nanoparticles with the four-different types of silane coupling agents (referred to as F0-OTS and F13-OTS).

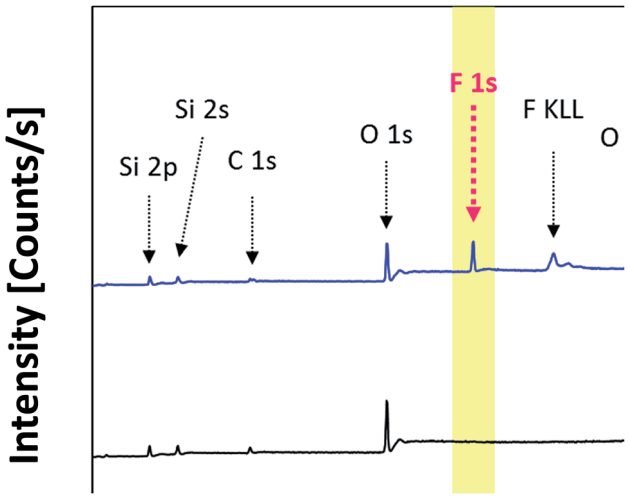

Fig. 1 Wide scan XPS spectra of the two-different hydrophobic surface modified Fe_3O_4@SiO_2 core–shell nanoparticles denoted as the Fe_3O_4@SiO_2-F0 and Fe_3O_4@SiO_2-F13, respectively.

the wide angle scan spectra reveal that silanization energies of ~284.5 eV and ~530.0 eV came from C 1s and O 1s. Moreover, a peak at around ~698.0 eV is clearly seen from the spectra that

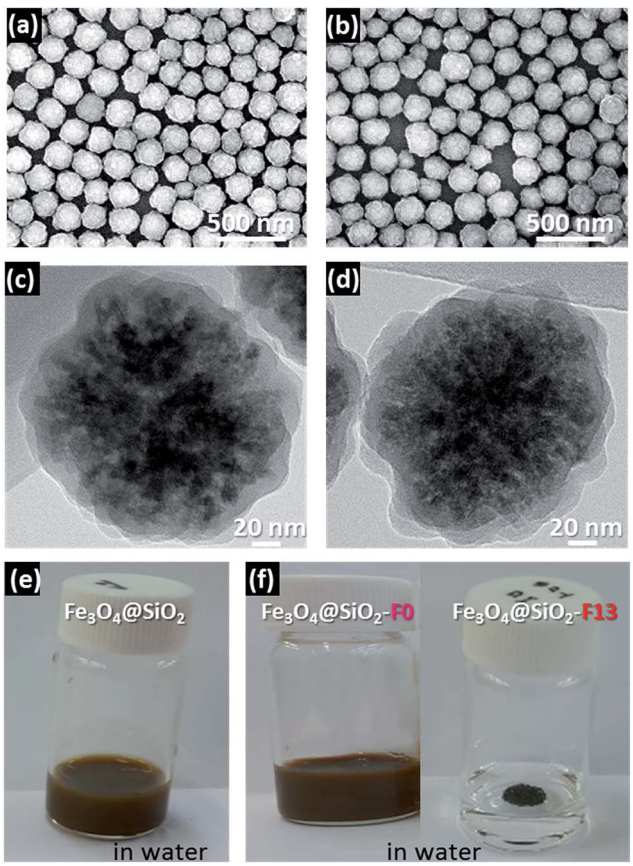

Fig. 2 (a and b) are the SEM images of the hydrophobic surface modified Fe_3O_4@SiO_2-F0 and Fe_3O_4@SiO_2-F13 core–shell nanoparticles, and (c and d) are the TEM images of their surrounding morphologies. (e and f) are the photo images showing different solubility behaviors.

corresponds to the F peak with the fluorine content in the Fe_3O_4@SiO_2-F13 core–shell nanoparticles, as expected.

The SEM, TEM, and solubility images are presented in Fig. 2. The SEM images in Fig. 2a and b show that the hydrophobic surface modified Fe_3O_4@SiO_2-F0 and Fe_3O_4@SiO_2-F13 core–shell nanoparticles have spherical shapes with a relatively narrow distribution size of ~180 nm. The TEM images of their surrounding morphologies are shown in Fig. 2c and d. However, it is difficult to distinguish the differences between the hydrophobic surface modified Fe_3O_4@SiO_2-F0 and Fe_3O_4@SiO_2-F13 core–shell nanoparticles with the SEM and TEM images. Therefore, the solubility in water for each hydrophobic surface modified Fe_3O_4@SiO_2-F0 and Fe_3O_4@SiO_2-F13 core–shell nanoparticle was investigated, and it was clearly confirmed that the surface modifications effectively occurred by silanization with different surface energies, shown in Fig. 2e and f.

In order to confirm whether the stimuli-responsive electrochromatic property of the two-different hydrophobic surface modified Fe_3O_4@SiO_2-F0 and Fe_3O_4@SiO_2-F13 core–shell nanoparticles precipitate out in a liquid, their dispersion stability was analyzed with zeta potential measurements both in EtOH and in a low dielectric medium (LDM). Table 1 shows the zeta potential values for the two-different hydrophobic surface modified Fe_3O_4@SiO_2-F0 and Fe_3O_4@SiO_2-F13 core–shell nanoparticles. The samples in the LDM had negative values of −62.9 and −78.0 mV for Fe_3O_4@SiO_2-F0 and Fe_3O_4@SiO_2-F13 core–shell nanoparticles, respectively, while the zeta potential values in EtOH have almost 2 times lower values, indicating that dispersion stability can be expected in the LDM and used in further investigations. Moreover, it is worth noting that when the zeta potential value of Fe_3O_4@SiO_2-F0 with the "no F moiety" is compared to that of the Fe_3O_4@SiO_2-F13 with the "F moiety" in each molecular structure, the negative zeta potential values for the "F moiety" in the molecular structure are higher which means the hydrophobic surface modified magnetite nanoparticles with the "F moiety" definitely affect the surface charges as well as the dispersion stability. It is clear that the "F moiety" molecular structure can improve the dispersion stability due to stronger interactions and an effective steric hindrance. Therefore, each ink of Fe_3O_4@SiO_2-F0 and Fe_3O_4@SiO_2-F13 was prepared for further investigation to examine the magneto-/electro-chromatic reflective optical properties.

Each prepared electro-chromatic ink for Fe_3O_4@SiO_2-F0 50 wt% and Fe_3O_4@SiO_2-F13 50 wt%, after adding a charge control agent (CCA) 10 wt% in LDM to increase the dispersion stability and to accelerate the stimuli-response under an applied voltage, was injected into the reflective display cell with a 100 μm thick gap. The magneto-/electro-chromatic reflective color-tunable properties were clearly observed when magnetic and electric fields were applied to the reflective display cell. Fig. 3 presents the photo images showing the appearance of the magneto-chromatic reflective color-changes in the reflective display cells before and after applying magnetic fields. Fig. 3a and b present the photo images showing the reflective rainbow color band referred to as the visible region. Fe_3O_4@SiO_2-F13 with the "F moiety" in the molecular structure displayed a better reflective rainbow color band than Fe_3O_4@SiO_2-F0 with the "no F moiety" in the molecular structure. Therefore, the hydrophobic surface modification with the "F moiety" in the molecular structure has an enhanced repulsion property to control the distance among the hydrophobic surface modified Fe_3O_4@SiO_2-F13 core–shell nanoparticles. However as shown in Fig. 3c, the reflective color-changes of the injected hydrophobic surface modified Fe_3O_4@SiO_2-F13 core–shell nanoparticle ink in the reflective display cell were not sufficient because the applied magnetic field may not have been strong enough. Furthermore, although the reflective color-changes were clearly detected, it was difficult to gradually control the reflective color change.

Therefore, in order to meet the "display application term", the electro-chromatic properties of the same hydrophobic

Table 1 Zeta potential of the four-different hydrophobic surface modified Fe_3O_4@SiO_2-F0 and Fe_3O_4@SiO_2-F13 core–shell nanoparticles in EtOH and in a low dielectric medium (LDM)

	Zeta potential [ξ, mV]	
	Fe_3O_4@SiO_2-F0	Fe_3O_4@SiO_2-F13
EtOH	−35.6	−39.2
LDM	−62.9	−78

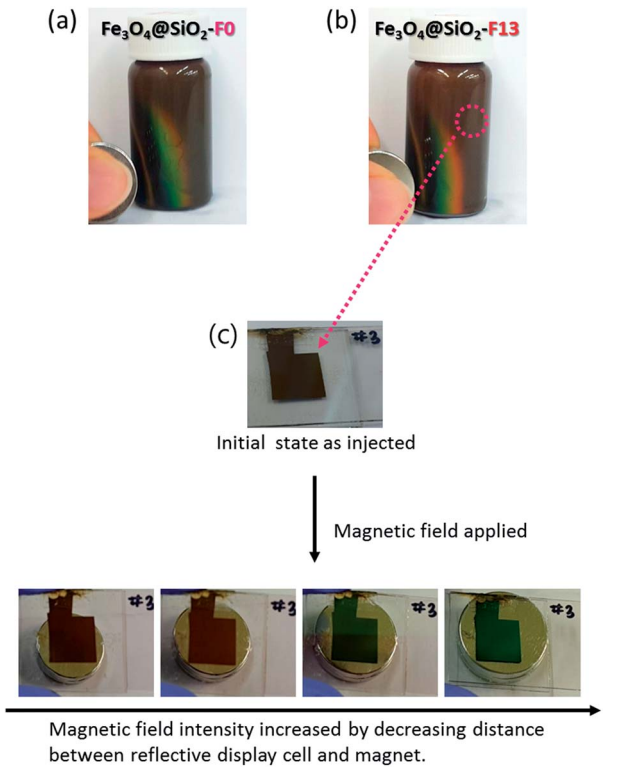

Fig. 3 [MAGNETO-CHROMATICS] photo images of the reflective color-changes of the hydrophobic surface modified (a) Fe_3O_4@SiO_2-F0 (with the "no F moiety" in the molecular structure) and (b) Fe_3O_4@SiO_2-F13 (with the "F moiety" in the molecular structure) core–shell nanoparticles under an applied magnetic field, and (c) reflective color-change behavior of the hydrophobic surface modified Fe_3O_4@SiO_2-F13 core–shell nanoparticle ink injected into the reflective display cells depending on the magnetic field intensity.

surface modified Fe_3O_4@SiO_2-F13 core–shell nanoparticles injected into the reflective display cell were examined to experimentally confirm the better magneto-chromic color-changes of the hydrophobic surface modified Fe_3O_4@SiO_2-F13 core–shell nanoparticles. After applying a voltage, shown in Fig. 4a, the hydrophobic surface modified Fe_3O_4@SiO_2-F13 core–shell nanoparticles moved towards the oppositely charged ITO electrode sites. By controlling the distance among the hydrophobic surface modified Fe_3O_4@SiO_2-F13 core–shell nanoparticles with increases or decreases of the electric field under applied voltages ranging from 0 V to 10 V, the reflective colors were gradually changed. Although the optical response of the electro-chromatic inks to the external electric field was very fast, less than 1 s, digital photo images were taken after a few seconds for every reflective color change in the electric field strength. The optical characteristics of the spectral variation in relation to the applied electric field are shown in Fig. 4b, measured in the diffuse mode. When applying an external electric field, the spacing between the charged nanoparticles is finely adjusted, and the reflected color shifts depend on the strength of the electric field. The reflected light can be continuously adjusted from light red by reducing the nanoparticle–nanoparticle distance by increasing the voltage gradually from 0 V to 10 V. To clearly observe the chromaticity of each reflective color of the hydrophobic surface modified Fe_3O_4@SiO_2-F13 core–shell nanoparticles, the international commission on illumination (CIE) chromaticity coordinates x and y were defined from each measured reflective color spectrum, and were calculated with the following equations:

$$x = X/(X + Y + Z);\ y = Y/(X + Y + Z);\ z = Z/(X + Y + Z) \quad (1)$$

where X, Y, and Z are well-known as the three tristimulus values. From the CIE chromaticity coordinates (0.475, 0.452) at 0 V, (0.503, 0.422) 0.9 V, (0.367, 0.507) 1.8 V, and (0.253, 0.248) at 8.8 V of the hydrophobic surface modified Fe_3O_4@SiO_2-F13 core–shell nanoparticles, corresponding to the initial color injected into the cell, reddish, greenish, and bluish colors, respectively, the color gamut can be visually displayed in the CIE 1931 chromaticity diagram shown in Fig. 4c. Although the color gamut of the reflective display cells with the hydrophobic surface modified Fe_3O_4@SiO_2-F13 core–shell nanoparticles seems low at 14.2%, the color gamut significantly improved by approximately two fold when the value was compared to the hydrophobic surface modified Fe_3O_4@SiO_2-F0 core–shell nanoparticles with the "no F moiety" in the molecular structure.

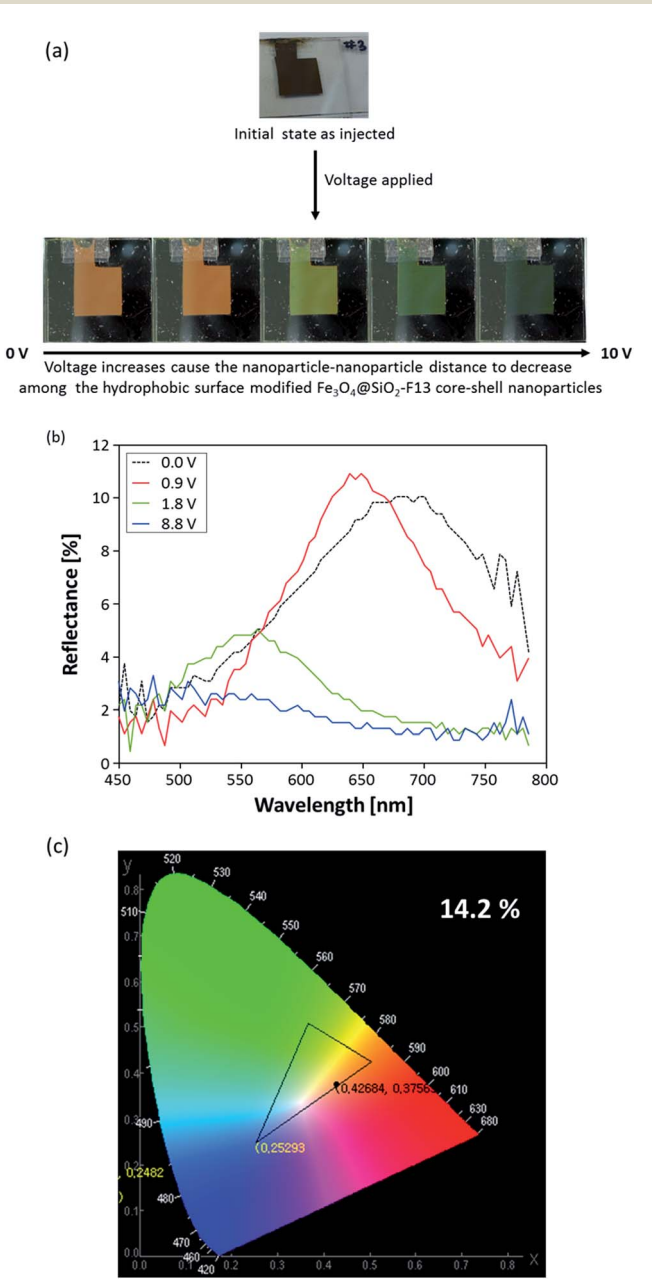

Fig. 4 [ELECTRO-CHROMATICS] (a) photo images of the reflective color-changes, (b) reflective color-change spectra, and (c) calculated color gamut (14.2%) presented in the CIE 1931 *xy* chromaticity diagram for the reflective display cells with the hydrophobic surface Fe_3O_4@SiO_2-F13 (with the "F moiety" in the molecular structure) core–shell nanoparticles under an applied voltage from 0 V to 10 V.

Conclusions

Two-different types of magneto-/electro-chromatic stimuli-responsive hydrophobic surface modified Fe_3O_4@SiO_2-Fx (x = 0 and 13) core–shell nanoparticles were successfully obtained. In order to investigate the potential for magneto-/electro-chromatic color-change, the hydrophobic surface modified Fe_3O_4@SiO_2-F0 and Fe_3O_4@SiO_2-F13 core–shell nanoparticles were effectively compared due to their molecular structural similarity with only one distinguishable difference between them: "no F moiety" and "F moiety" in their molecular structure, respectively. From the investigation of the magneto-chromatic properties, it was clearly observed that the "F moiety" in the molecular structure of hydrophobic surface modified Fe_3O_4@SiO_2-Fx core–shell nanoparticles improves the color-change spectrum in the visible region while the "no F moiety" in the molecular structure has a worse color-change band. Moreover, on examination of the electro-chromatic properties, the color-gamut of the hydrophobic surface modified Fe_3O_4@SiO_2-F13 core–shell nanoparticles with the "F

moiety" in the molecular structure is significantly enhanced by approximately two fold when the value is compared to that of the hydrophobic surface modified Fe_3O_4@SiO_2-F0 core–shell nanoparticles with the "no F moiety" in the molecular structure. Therefore, hydrophobic surface modified Fe_3O_4@SiO_2-F*x* core–shell nanoparticles with an "F moiety" in the molecular structure can be potentially considered for application in a reflective display.

Experimental

Materials

A silica coated magnetic Fe_3O_4 core–shell nanoparticle dispersion (Fe_3O_4@SiO_2, MTX ink) with an average particle size of 180 nm was purchased from Nanobrick Co. (Korea). Ethanol (EtOH) was purchased from Dongwoo FineChem Co. Ltd. (Korea). Ammonia solution (NH_3, 28–30 wt%) was purchased from Samchun Pure Chemical Co. Ltd. (Korea). Octyltriethoxysilane (F0-OTS, 98%) and 1*H*,1*H*,2*H*,2*H*-perfluorooctyltriethoxysilane (F13-OTS, 98%) were purchased from Sigma-Aldrich (USA). All reagents were used as received.

Hydrophobic surface modification of Fe_3O_4@SiO_2 (referred to as Fe_3O_4@SiO_2-F*x*, $x = 0$ and 13)

One gram of Fe_3O_4@SiO_2 core–shell nanoparticles and 300 mL of ethanol were added to a baffled double-jacket flask and the mixture was dispersed with ultra-sonication (700 W, ULH 700S, Ulsso Hitech Co., Ltd.) for 2 h. Then, 10 mL of ammonia solution were added to the flask to adjust the pH to almost 11. Then, 1.6 mM of the two different types of silane coupling agents, denoted as F0-OTS and F13-OTS, were slowly added to this mixture and the solution was heated for 24 h at 50 °C. After cooling to room temperature, the reacted mixture was centrifuged at 7000 rpm and washed with EtOH. These processes were repeated at least 3 times to remove any excess silane coupling agent. After vacuum freeze-drying, the hydrophobic treated Fe_3O_4@SiO_2 core–shell nanoparticles (referred to as Fe_3O_4@SiO_2-F0 and Fe_3O_4@SiO_2-F13) were obtained.

Characterization

The reaction for Fe_3O_4@SiO_2-F0 and Fe_3O_4@SiO_2-F13 core–shell nanoparticles was confirmed by analyzing their chemical information and quantitative elements using an X-ray photoelectron spectrometer (XPS, MultiLab 2000, Thermo Fischer Scientific, USA) with a monochromatic Al Kα source. Morphological images were obtained with transmission electron microscopy (JEOL 200CX, USA). To determine the sizes and surface morphologies, scanning electron microscopy (SEM) was used in the secondary electron imaging mode at 10 keV with a high resolution FE-SEM (Sirion 400, USA) and a transmission electron microscope (TEM, JEOL 200CX, Japan) operated at 300 kV. The zeta potential was determined with a zeta potential analyzer (Nano ZS90, Malvern Instruments Ltd., UK). The reflectance spectra and color coordinates were measured using a LCD electro-optical measurement system (LCD 5200, Otsuka Electronics Co., Ltd., JP) with $BaSO_4$ as the reference, and their optical changes were detected with a fixed angle gap of 20° between the incident light and reflected light.

Preparation of reflective color-tunable display cells

First, an ITO glass slide was cut into 2 cm × 3 cm pieces. The pieces were cleaned in an ultra-sonic bath with isopropyl alcohol (IPA) and deionized (DI) water followed by drying with N_2 gas. The ITO glass pieces were placed with the ITO sides face-to-face and sealed with a 100 μm thick thermal adhesive tape. Then, magneto-/electro-chromatic ink, which was a mixture of each of the hydrophobic Fe_3O_4@SiO_2-F0 and Fe_3O_4@SiO_2-F13 core–shell nanoparticles mixed with a dispersing agent in a low dielectric medium, was injected into the cells.

Acknowledgements

This work was supported by Korea Evaluation Institute of Industrial Technology (KEIT) grant funded by the Korea government (MOTIE) (No. 10041221, Development of the colloidal photonic crystal film for full-color tuning electronic skins.) and Institute for Information & communications Technology Promotion (IITP) grant funded by the Korea government (MSIP) (B0101-16-0133, The core technology development of light and space adaptable energy-saving I/O platform for future advertising service).

References

1 J. Y. Kim, C. W. Joo, J. Lee, J.-C. Woo, J.-Y. Oh, N. S. Baek, H. Y. Chu and J.-I. Lee, *RSC Adv.*, 2015, **5**, 8415–8421.
2 C. Murawski, K. Leo and M. C. Gather, *Adv. Mater.*, 2013, **25**, 6801–6827.
3 C. A. Smith, *Circuit World*, 2008, **34**, 35–41.
4 J. Heikenfeld, P. Drzaic, J.-S. Yeo and T. Koch, *J. Soc. Inf. Disp.*, 2011, **19**, 129–156.
5 J. Y. Kim, J.-Y. Oh and K.-S. Suh, *Carbon*, 2014, **66**, 361–368.
6 J. Y. Kim, J.-Y. Oh, S. Cheon, H. Lee, J. Lee, J.-I. Lee, H. Ryu, S. M. Cho, T.-Y. Kim, C.-S. Ah, Y.-H. Kim and C.-S. Hwang, *Opt. Mater. Express*, 2016, **6**, 3127–3134.
7 Z. J. Luo, W. N. Zhang, L. W. Liu, S. Xie and G. Zhou, *J. Soc. Inf. Disp.*, 2016, **24**, 345–354.
8 J. D. Joannopoulos, S. Johnson, J. Winn and R. Meade, *Photonic Crystals: Molding the Flow of Light*, Princeton University Press, Princeton, New Jersey, USA, 2008.
9 H. S. Lee, T. S. Shim, H. Hwang, S.-M. Yang and S.-H. Kim, *Chem. Mater.*, 2013, **25**, 2684–2690.
10 C. G. Schäfer, M. Gallei, J. T. Zahn, J. Engelhardt, G. P. Hellmann and M. Rehahn, *Chem. Mater.*, 2013, **25**, 2309–2318.
11 M. Xiao, Y. Li, J. Zhao, Z. Wang, M. Gao, N. C. Gianneschi, A. Dhinojwala and M. D. Shawkey, *Chem. Mater.*, 2016, **28**, 5516–5521.
12 L. Babes, B. t. Denizot, G. Tanguy, J. J. Le Jeune and P. Jallet, *J. Colloid Interface Sci.*, 1999, **212**, 474–482.

13 I. Chourpa, L. Douziech-Eyrolles, L. Ngaboni-Okassa, J.-F. Fouquenet, S. Cohen-Jonathan, M. Souce, H. Marchais and P. Dubois, *Analyst*, 2005, **130**, 1395–1403.
14 T. K. Jain, M. A. Morales, S. K. Sahoo, D. L. Leslie-Pelecky and V. Labhasetwar, *Mol. Pharm.*, 2005, **2**, 194–205.
15 C.-L. Li, J.-K. Chen, S.-K. Fan, F.-H. Ko and F.-C. Chang, *ACS Appl. Mater. Interfaces*, 2012, **4**, 5650–5661.
16 C.-L. Li, C.-J. Chang and J.-K. Chen, *Sens. Actuators, B*, 2015, **210**, 46–55.
17 C.-L. Li, B.-R. Huang, J.-Y. Chang and J.-K. Chen, *J. Mater. Chem. C*, 2015, **3**, 4603–4615.
18 M. G. Han, C.-J. Heo, H. Shim, C. G. Shin, S.-J. Lim, J. W. Kim, Y. W. Jin and S. Lee, *Adv. Opt. Mater.*, 2014, **2**, 535–541.
19 I. Lee, D. Kim, J. Kal, H. Baek, D. Kwak, D. Go, E. Kim, C. Kang, J. Chung, Y. Jang, S. Ji, J. Joo and Y. Kang, *Adv. Mater.*, 2010, **22**, 4973–4977.
20 T. S. Shim, S.-H. Kim, J. Y. Sim, J.-M. Lim and S.-M. Yang, *Adv. Mater.*, 2010, **22**, 4494–4498.
21 L. Nucara, F. Greco and V. Mattoli, *J. Mater. Chem. C*, 2015, **3**, 8449–8467.
22 L. Zhuang, Y. Zhao, H. Zhong, J. Liang, J. Zhou and H. Shen, *Sci. Rep.*, 2015, **5**, 17063.